



Metabolomic profiling and molecular docking study of mucus from the Indonesian land snail *Hemiplecta humphreysiana* Lea, 1840 (Gastropoda) to unveil its potential as an anti-tyrosinase and an anti-elastase agent

Ukhradiya M. S. Purwanto^a, Pamungkas R. Ferdian^b, Paradisica Paradisica^a, Rizki R. Elfirta^c, Ayu S. Nurinsiyah^d, Ikhsan Guswenrivo^b, Laksmi Ambarsari^a

^aDepartment of Biochemistry, Faculty of Mathematics and Natural Sciences, Bogor Agricultural University (IPB University),

^bResearch Center for Applied Zoology,

^cResearch Center for Applied Microbiology,

^dResearch Center for Biosystematics and Evolution, National Research and Innovation Agency of Indonesia, Cibinong, Bogor, West Java, Indonesia

Correspondence to Ukhradiya M. S. Purwanto, MSc, Department of Biochemistry, Faculty of Mathematics and Natural Sciences, Bogor Agricultural University (IPB University), 16680, Bogor, West Java, Indonesia.
Tel and Fax: +62 0251 8423267;
e-mail: irabikg8@apps.ipb.ac.id

Received: 1 July 2024

Revised: 26 August 2024

Accepted: 27 August 2024

Published: 17 December 2024

Egyptian Pharmaceutical Journal 2025,
24: 100–121

Background

Mucus from several species of snails has been known to contain bioactive compounds such as anti-tyrosinase and anti-elastase. These two compounds contribute as whitening agents and anti-wrinkle agents, respectively. Among the many land snail species in Indonesia, only one species, *Lissachatina fulica*, has been analyzed for its bioactive compound. This species is an invasive alien species and non-native to Indonesia. In this study, we aim to unravel the bioactive compounds in one Indonesian native species, *Hemiplecta humphreysiana*.

Objective

To identify bioactive compounds in the mucus of *H. humphreysiana* using ultra-performance liquid chromatography-mass spectrometry/mass spectrometry quadrupole time-of-flight (UPLC-MS/MS QTOF) and to evaluate their potential as anti-tyrosinase and anti-elastase agents using molecular docking.

Materials and methods

Carbonate buffer at pH 9.4 was used to extract mucus from *H. humphreysiana* snails. Lyophilized mucus samples were dissolved in methanol and dichloromethane solvents, filtered, and injected into a UPLC-MS/MS instrument. The data analysis was conducted using MassLynx software. The molecular formulas and spectra were compared with databases such as ChemSpider, PubChem, MassBank, Human Metabolome Database, and the National Institute of Standards and Technology to obtain the metabolomic profile of the sample. Bioactive metabolites were evaluated for ligand–protein interactions using a molecular docking approach with AutoDock tools and AutoDock Vina. Results were visualized in two-dimensional and three-dimensional using Discovery Studio and analyzed for bond affinity energy. Scoring was conducted to identify potential inhibitors of tyrosinase or elastase.

Results and conclusion

A total of bioactive compounds were identified from the mucus of *H. humphreysiana* Lea, 1840. Twenty compounds were identified as suspected compounds, and 13 were confirmed. Based on the bioavailability and toxicity characteristics, analysis of affinity energy, and ligand–receptor interaction, about 13 compounds can inhibit tyrosinase, and 12 compounds can inhibit elastase. Indoleacrylic acid and withanone were determined to be lead compounds with anti-tyrosinase activity, while withanone and 7-[2-(1-adamantyl)-2-oxoethyl]-1,3-dimethyl-8-(4-methylpiperazin-1-yl) purine-2,6-dione were identified as lead compounds as anti-elastase agents. Metabolomic profiling using UPLC-MS/MS QTOF can identify bioactive compounds for use as test ligands in molecular docking. The presence of lead compounds in *H. humphreysiana* mucus to inhibit tyrosinase and elastase shows its potential as a whitening and anti-wrinkle agent, respectively. This study initiates the bioprospecting of *H. humphreysiana* mucus as nutraceuticals for future research.

Keywords:

bioprospecting, *Hemiplecta humphreysiana*, metabolomic, molecular docking, natural product

EgyptPharmaceutJ24:100–121

©2025 Egyptian Pharmaceutical Journal

1687-4315

Introduction

The use of snails (mollusk: gastropoda) in daily life is common for local people in Indonesia. The snails are often used for human consumption, animal feed, and

traditional medicine [1]. The snails have now become a global trend. The mucus of land snails is now being used as the base ingredient for nutriscosmeceutical. Nutriscosmeceutical is an industrial term obtained by combining “nutraceuticals” and “cosmeceuticals” to describe supplements, functional foods, and drinks that contain active ingredients for beauty and health [2]. According to transparency market research [3], skin care dominates the nutriscosmetics market with an expected growth rate of 4.5% compound annual growth rate to reach \$194.961 million in 2024, and with a projected 5% compound annual growth rate, the market is expected to be worth US\$7.93 billion by 2025. Along with the increasing demand for natural cosmetics, there has been an increase in the global market for beauty products with natural raw materials. One of the natural raw materials used for beauty products is snails, taking their extract, mucus, oil, serum, or filtrate.

The part of the snail most used as a natural raw material for beauty products is snail mucus, which can stimulate the formation of collagen, elastin, and dermal components, improving signs of photoaging and reducing damage produced by free radicals [4]. The snail mucus reportedly contains an active mixture of substances such as allantoin, collagen, elastin, and glycolic acid along with glycoproteins (mucin) and mucopolysaccharides, which are generally considered useful in the treatment of skin disorders [5]. Allantoin, or 5-ureidohydantoin, is one of several uric acid oxidation products that is safe and effective for use as a raw material for skin protection [6,7]. Allantoin helps fight skin damage because it has a desquamating action and helps cell proliferation and wound healing. Allantoin can be used in personal care products and cosmetics such as shampoo, lotion, cream, lipstick, anti-acne products, and others because allantoin can bind the water content of the extracellular matrix and form complexes with irritating and sensitizing substances [8].

The snail mucus can act as a tyrosinase and elastase inhibitor [9,10]. Tyrosinase inhibition is popular in the beauty and medical fields because it can prevent melanogenesis (the process of melanin biosynthesis) by inhibiting enzymatic oxidation. Tyrosinase inhibitors can brighten the skin by reducing the effect of skin darkening, as the melanogenesis mechanism is inhibited, thereby preventing melanin hyperpigmentation [11]. Meanwhile, elastase plays a role in degrading elastin in the skin. The damage to elastin fibers causes skin elasticity to decrease [12]. Elastase activity increases significantly with age and is

also caused by the presence of free radicals, thereby reducing the elasticity of the skin, and making the skin appear aged and withered. Elastase has a significant impact on the metabolism of elastic fibers in skin tissue during photoaging [13]. Inhibition of elastase is currently a trend in the beauty sector because it can inhibit the process of elastin degradation, which can maintain skin elasticity and prevent skin from wrinkling.

The global use of land snail mucus is still limited to a few species, such as *Helix aspersa* (*Cornu aspersum*), *Lissachatina fulica*, and *Hemiplecta distincta* [1]. The mucus of the land snail *H. aspersa* can inhibit tyrosinase activity and melanin production in cell lines [14]. *H. distincta*, a land snail from Thailand, also produces mucus which exhibits anti-tyrosinase as well as antioxidant activity [15]. In Sumatra and Java, there are at least 280 and 263 land snail species, respectively [16,17]. Indonesia, especially Java, is not the natural distribution area of *H. aspersa*. The species is naturally distributed in Europe. *L. fulica* is an invasive alien species that is found abundantly in human-modified habitats. Java, the most populated island in Indonesia, is covered by large areas of human-modified habitat. The presence of *L. fulica* is common on the island. Meanwhile, *H. distincta* has not been recorded in Java. However, *H. humphreysiana*, a sister species of *H. distincta*, can be found in agroforests and plantations with good canopy coverage in Java.

H. humphreysiana has a relatively large body (about 5 cm in size) and can produce a good amount of mucus [18,19]. This species has the potential to be developed for nutriscosmeceutical products. Therefore, the identification of bioactive compounds from *H. humphreysiana* mucus and their effects on skin health and beauty needs to be conducted to enter the nutriscosmeceutical market. This research aims to identify bioactive compounds in the mucus of *H. humphreysiana* using ultra-performance liquid chromatography-mass spectrometry/mass spectrometry quadrupole time-of-flight (UPLC-MS/MS QTOF) and to unveil their potential as anti-tyrosinase and anti-elastase agents using molecular docking.

Materials and methods

Samples collection

The land snail samples of *H. humphreysiana* were collected from Menoreh, Yogyakarta, Indonesia. These samples were transported to the laboratory for molluscs and other invertebrates at the National Research and Innovation Agency of Indonesia. The

snails were housed in a ventilated box (36×28×13 cm) filled with garden soil and small rocks to mimic their natural habitat. The box was sprayed with water twice daily to maintain humidity. It was placed in the room with an air conditioner set to 25°C and 70–80% humidity. During the experiment, the snails were fed a diet of oyster mushrooms (*Pleurotus ostreatus*), cucumbers (*Cucumis sativus*), and papayas (*Carica papaya*) [1,18].

Mucus extraction

The mucus extraction involved stimulating the snails with a carbonate buffer at pH 9.4 for 30 min, inducing mucus production without harm. The mucus was then filtered through glass wool to remove contaminants and freeze-dried for storage.

Metabolomic profiling

Lyophilized mucus samples were dissolved in methanol and dichloromethane (DCM) to a concentration of 1000 µg/ml, filtered, and injected into a UPLC-MS/MS instrument. The mobile phase consisted of 5 mM ammonium formate in H₂O and 0.05% formic acid in acetonitrile, with a flow rate of 0.20 ml/min and a column temperature of 50°C. A C18 HSS T3 1.8 µm column and QTOF detector with ESI were used. Data analysis was conducted using MassLynx software. After that, the molecular formulas and spectra were compared with databases such as ChemSpider, PubChem, MassBank, Human Metabolome Database, and National Institute of Standards and Technology to obtain the metabolomic profile of the sample.

Prediction of bioavailability and toxicity ligands

The ligands were further evaluated for their similarity to drug-like compounds using the Lipinski Rule of Five, which can be accessed at <http://scfbio-iitd.res.in/software/drugdesign/lipinski.jsp>. The compounds that met the Lipinski criteria were subsequently subjected to toxicity prediction tests. The ligands, in SMILES format, previously obtained using the ChemSketch software, were used to predict toxicity values, accessible at admetSAR (<http://lmmd.ecust.edu.cn/admetSar1/predict/>). The toxicity parameters analyzed included inhibition of the human ether-a-go-go-related gene, carcinogenicity, and acute oral toxicity. Predictions for skin sensitization were carried out using the database available on the pKCSM website.

Molecular docking

Molecular docking assessed ligand–protein interactions, focusing on binding affinity. The steps

included ligand and receptor preparation, validation, docking, visualization, and scoring. Ligands were reconstructed using ChemSketch and saved in *MOL and *SMILE formats, converted to *PDB and *PDBQT formats using Discovery Studio and AutoDock tools. Receptors (tyrosinase, PDB ID: 6EI4; elastase, PDB ID: 4YM9) were prepared by removing water, heteroatoms, and complex ligands, then saved in *PDB format and converted to *PDBQT with hydrogen added to polar parts and Gasteiger charges calculated. Natural ligands B5N and 4E4 were separated from receptors and prepared similarly.

The docking was validated by redocking natural ligands and assessing RMSD values, with RMSD less than 2 Å considered valid. Molecular docking was performed using AutoDock tools and AutoDock Vina, with specific grid box settings for each receptor. Results were visualized in Discovery Studio and analyzed for bond affinity energy.

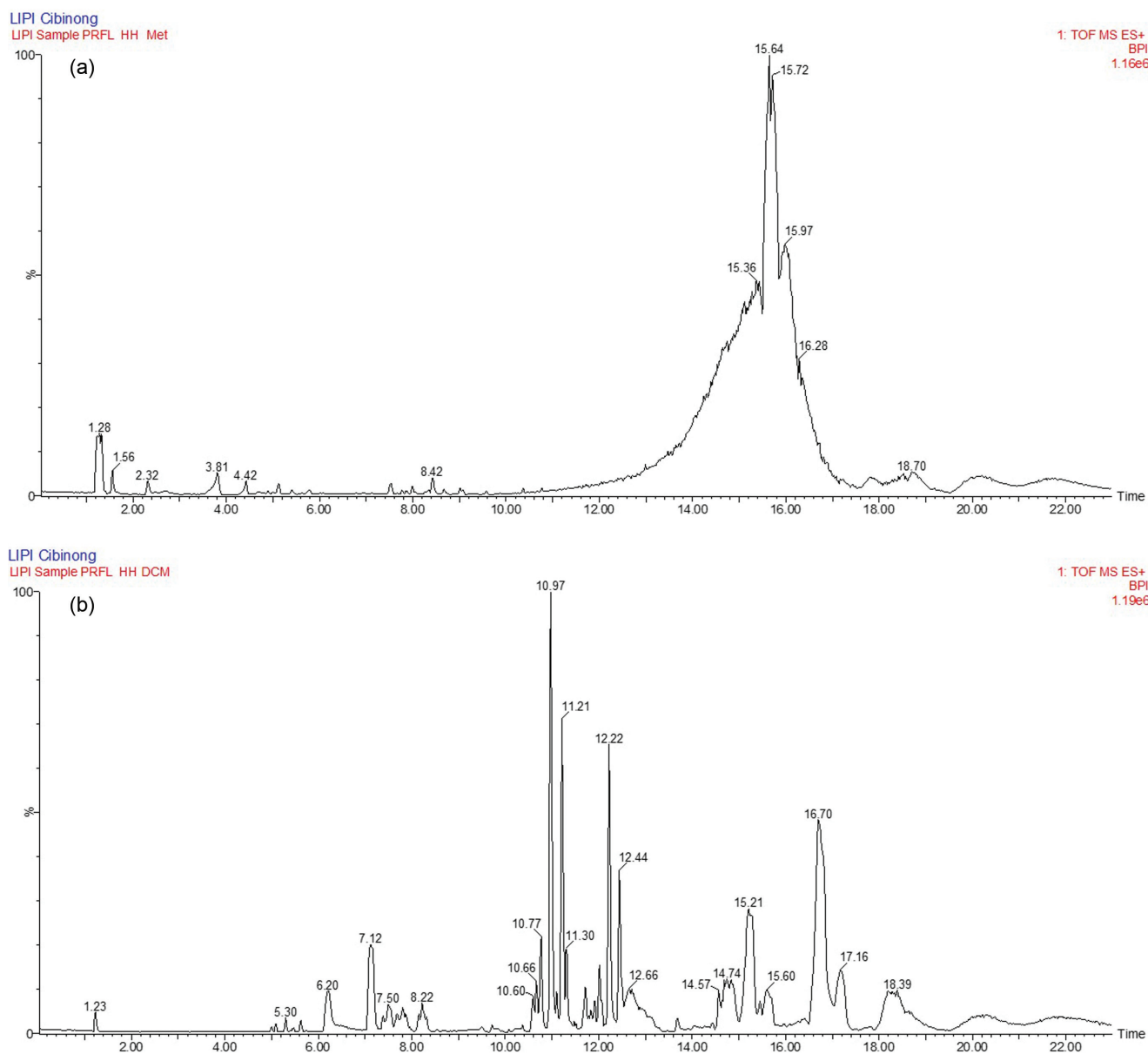
Visualization and scoring

The docking results were visualized in two-dimensional (2D) and three-dimensional (3D) using Discovery Studio. The 3D visualization showed ligand binding sites on receptors, while 2D analyzed molecular interactions such as hydrogen bonds and hydrophobic interactions. Scoring considered affinity energy and inhibition area, comparing the test ligand's affinity energy and the number of interacting amino acid residues with those of comparison ligands. The final score averaged these percentages, identifying potential inhibitors of tyrosinase or elastase.

Results and discussions

The chromatogram data from UPLC-MS/MS analysis showed 33 compounds from two types of solvents (methanol and DCM) (Fig. 1). Among these, 20 compounds are suspected compounds, and 13 compounds are confirmed compounds (Tables 1 and 2). The suspected compounds were identified by molecular formulas and parent ion spectra from low-energy spectrometry systems and matched with databases such as ChemSpider or PubChem. Meanwhile, the confirmed compounds were those among the suspected compounds. The isomers were confirmed by analyzing the daughter ion(s) spectra from the medium-energy spectrometry system and comparing them with the spectra on the MassBank, Human Metabolome Database, and National Institute of Standards and Technology databases. These bioactive compounds were used as test ligands in

Figure 1

Chromatogram of *Hemiplecta humphreysiana* Lea, 1840 mucus with (a) methanol solvent and (b) dichloromethane (DCM) solvent.

this study. The compounds with the highest abundance were di(2-ethylhexyl)-phthalate (methanol solvent) and 4,4'-bis(1-phenylmethyl) diphenylamine (DCM solvent).

The crystal structure of the tyrosinase receptor (PDB ID: 6EI4) and elastase receptor (PDB ID: 4YM9) was used in previous studies [19,20]. The crystal structure of tyrosinase (PDB ID: 6EI4) was deposited by Ferro *et al.* [21] with a resolution of 2.00 Å. The secondary structure of the receptor obtained from <https://www.rcsb.org/sequence/6EI4> shows the active site area, which includes residues His42, Val218, Arg209, His208, Pro201, His204, His231, His69, and His60. The binding area of the B5N inhibitor on the active site of the tyrosinase is predominantly

covered by hydrophobic interactions formed with amino acid residues Val218, His208, Arg209, and Pro201. However, the crystal structure of elastase (PDB ID: 4YM9) was deposited by Ruivo *et al.* [22] with a resolution of 1.80 Å. Its secondary structure shows the active site area, including residues His57, Gly193, Ser195, and Ser214. The binding area of the 4E4 inhibitor on the active site of the elastase is predominantly covered by hydrogen bonds with amino acid residues Gly193 and Ser195. The ligand binding to the active site inhibits the receptor's action because the enzyme's substrates cannot attach to the active site [23].

The receptor stability is an important factor that must be ensured before running molecular docking. As the

Table 1 Bioactive compounds in *Hemiplecta humphreysiana* Lea, 1840 mucus as a result of ultra-performance liquid chromatography-mass spectrometry/mass spectrometry quadrupole time-of-flight analysis with methanol solvent

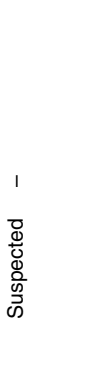
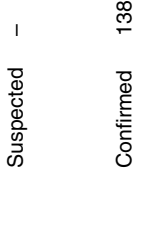


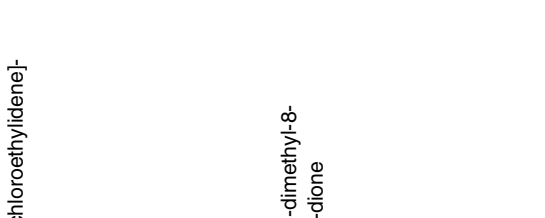
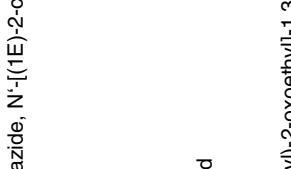
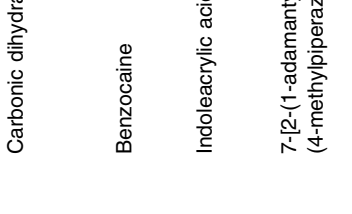
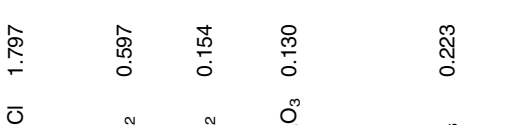
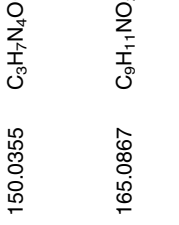
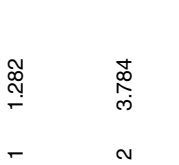
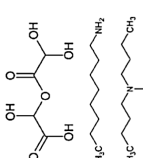
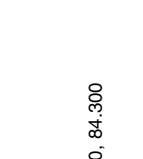
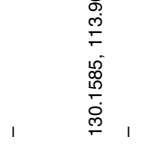
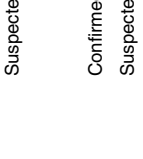
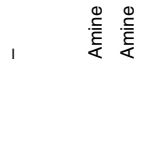


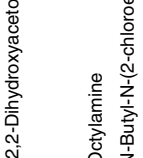
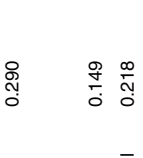
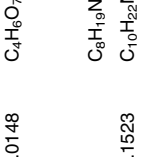
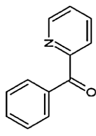
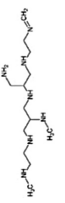
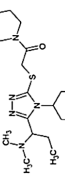

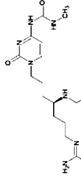
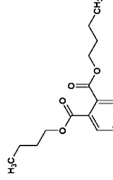
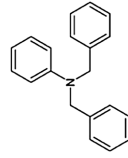
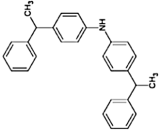
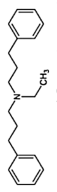
No	Retention time (min)	Molecular weight (Da)	Molecular formula	Abundance (%)	Compound	Class of bioactive compound	Compound status	Confirmed daughter ion	Molecular structure
1	1.282	150.0355	C ₃ H ₇ N ₄ OCl	1.797	Carbonic dihydrazide, N'-[(1E)-2-chloroethylidene]-	Amine	Suspected	-	
2	3.784	165.0867	C ₉ H ₁₁ NO ₂	0.597	Benzocaine	Alkaloid	Confirmed	138.0555, 120.0807, 92.1740	
3	4.424	187.0713	C ₁₁ H ₉ NO ₂	0.154	Indoleacrylic acid	Alkaloid	Confirmed	115.0534, 138.0546, 118.0655, 91.0544, 70.0646	
4	7.517	454.2802	C ₂₄ H ₃₄ N ₆ O ₃	0.130	7-[2-(1-adamanty)-2-oxoethyl]-1,3-dimethyl-8-(4-methylpiperazin-1-yl)purine-2,6-dione	Alkaloid	Suspected	-	
5	8.417	470.2773	C ₂₈ H ₃₈ O ₆	0.223	Withanone	Glycerophospholipids	Confirmed	435.2544, 237.1138, 283.2713, 181.1010, 171.1172, 159.1166	
6	15.694	390.288	C ₂₄ H ₃₈ O ₄	89.11	Di(2-ethylhexyl)phthalate	Ester	Confirmed	149.0252, 121.0296, 65.0389	
7	17.845	428.3729	C ₂₉ H ₄₈ O ₂	0.608	Cholesteryl acetate	Steroid	Confirmed	327.0768, 95.0854, 109.1013, 175.1478, 107.0853	
8	18.745	534.4921	C ₃₈ H ₆₂ O	1.899	(5E,9E,13E,17E,21E,25E)-6,10,14,18,22,26,30-Heptamethyl-5,9,13,17,21,25,29-hentriacontahptaen-2-one	-	Suspected	-	
9	20.172	181.9813	CH ₂ N ₄ O ₅ S	2.563	Azanylidyne-[hydroxysulfamoyl(nitro)amino]methane	-	Suspected	-	
10	21.712	181.9855	C ₂ H ₂ N ₂ O ₈	2.347	(Carbonoperoxyloxydiazeny) hydroxy carbonate	-	Suspected	-	

Table 2 Bioactive compounds of *Hemiplecta humphreysiana* Lea, 1840 mucus as a result of ultra-performance liquid chromatography-mass spectrometry/mass spectrometry quadrupole time-of-flight analysis with dichloromethane solvent

No	Retention time (min)	Molecular weight (Da)	Molecular formula	Abundance (%)	Compound	Class of bioactive compound	Compound status	Confirmed daughter ion	Molecular structure
1	1.232	166.0148	C ₄ H ₆ O ₇	0.290	(2,2-Dihydroxyacetoxy)(hydroxy)acetic acid	-	Suspected	-	
2	5.077	129	C ₈ H ₁₉ N	0.149	Octylamine	Amine	Confirmed	130.1585, 113.9620, 84.300	
3	5.626	191.1523	C ₁₀ H ₂₂ NCl	0.218	N-Butyl-N-(2-chloroethyl)-1-butanamine	Amine	Suspected	-	
4	6.224	224.1392	C ₁₅ H ₁₆ N ₂	2.226	N,N-Dimethyl-4-[(E)-2-(4-pyridinyl)vinyl] aniline	Alkaloid	Suspected	-	
5	7.124	183.1001	C ₉ H ₁₃ NO ₃	3.970	(-)-Epinephrine	Alkaloid	Confirmed	107.0606, 166.300	
6	7.496	265.1657	C ₁₇ H ₁₉ N ₃	1.205	Mirtazapine	Alkaloid	Confirmed	223.1100, 209.0971	
7	7.806	311.15	C ₁₈ H ₂₁ N ₃ S	1.092	(2E)-2-(Mesitylmethylene)-N-(3-methylphenyl)hydrazinecarbothioamide	Alkaloid	Suspected	-	
8	8.22	287.2892	C ₁₇ H ₃₇ NO ₂	1.024	2,2'-(Tridecylimino)diethanol	Amine	Suspected	-	
	10.752	287.2901		2.783					
	10.97	287.2915		10.047					
9	9.451	339.186	C ₂₀ H ₂₅ N ₃ S	0.211	Perazine	Alkaloid	Confirmed	255.0918, 86.0950	
10	9.76	269.1055	C ₁₅ H ₁₅ N ₃ S	0.174	2-Amino-6-benzyl-3-cyano-4,5,6,7-tetrahydrothieno[2,3-c]pyridine	Alkaloid	Suspected	-	


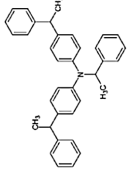
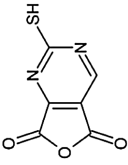
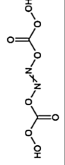
(Continued)

Table 2 (Continued)

No	Retention time (min)	Molecular weight (Da)	Molecular formula	Abundance (%)	Compound	Class of bioactive compound	Compound status	Confirmed daughter ion	Molecular structure
11	10.308	183.0769	C ₁₂ H ₉ NO	0.101	Phenyl(2-pyridinyl)methanone	Alkaloid	Confirmed	149.0239, 128.0631, 156.0894	
12	11.229	287.2844	C ₁₃ H ₃₃ N ₇	7.139	2-N-[2-(methylamino)-3-[2-(methylamino)ethylamino]propyl]-3-N-[2-(methylideneamino)ethyl]propane-1,2,3-triamine	Amine	Suspected	–	
13	11.736	395.2422	C ₁₉ H ₃₃ N ₆ O ₂ S	1.114	2-[(4-Cyclohexyl)-5-[1-(dimethylamino)propyl]-4H-1,2,4-triazol-3-yl]sulfany]-1-(4-morpholinyl)ethanone	Alkaloid	Suspected	–	
14	12.221	315.3179	C ₁₉ H ₄₁ NO ₂	7.959	1-hexadecyl-2-amino-2-deoxy-sn-glycerol	Amine	Suspected	–	
15	12.46	315.3208		7.426					
15	14.091	451.3217	C ₁₉ H ₃₇ N ₁₁ O ₂	0.223	1-[1-[(4S)-7-(diaminomethylideneamino)-4-[4-(diaminomethylideneamino)butylamino]heptyl]-2-oxopyrimidin-4-yl]-3-methylurea	Alkaloid	Suspected	–	
16	14.795	278.1599	C ₁₆ H ₂₂ O ₄	5.427	Dibutyl phthalate	Ester	Confirmed	149.0234, 121.0285, 105.0334, 57.0700	
17	15.23	273.1583	C ₂₀ H ₁₉ N	8.753	Benzenemethan amine	Alkaloid	Confirmed	182.0974, 180.0792, 105.0740, 165.0703, 167.0738, 196.1105	
18	15.602	273.1582		2.361					
18	16.749	377.2192	C ₂₈ H ₂₇ N	17.359	4,4'-Bis(1-phenylethyl)diphenylamine	Alkaloid	Suspected	–	
19	17.163	281.2204	C ₂₀ H ₂₇ N	4.187	Alverine	Alkaloid	Suspected	–	

(Continued)

Table 2 (Continued)

No	Retention time (min)	Molecular weight (Da)	Molecular formula	Abundance (%)	Compound	Class of bioactive compound	Compound status	Confirmed daughter ion	Molecular structure
20	17.782	328.3206	C ₂₀ H ₄₁ NO ₂	0.103	N,N-Dimethylsphingosine	Amine	Confirmed	266.9983, 223.0623	
21	18.281	481.2853	C ₃₈ H ₃₅ N	6.572	N,4-Bis(1-phenylethyl)-N-[4-(1-phenylethyl)phenyl]aniline	Alkaloid	Suspected	–	
22	20.264	181.983	C ₆ H ₂ N ₂ O ₃ S	3.863	2-Sulfanylfur[3,4-d]pyrimidine-5,7-dione	Alkaloid	Suspected	–	
23	21.846	181.9857	C ₂ H ₂ N ₂ O ₈	3.499	(Carbonoperoxyoxydiazeny) hydroxy carbonate	–	Suspected	–	

results of molecular docking are predictive, all instruments, including receptor stability, must be well-prepared to ensure that the results are as close as possible to real conditions. Two parameters can be used to determine the receptor stability: resolution and the Ramachandran plot of the receptor [23]. A receptor can be considered stable if its resolution is less than 2.5 Å and the disallowed region on the Ramachandran plot is less than 15% [23–25]. Both receptors in the present study have a resolution of less than 2.5 Å and can be considered stable. The Ramachandran plot of tyrosinase (PDB ID: 6E14) is shown in Fig. 2a, indicating that 97.7% (558/571) of all residues are in the favored regions, 100.0% (571/571) are in the allowed regions, and 0 (0.0%) are in the disallowed regions. The Ramachandran plot of elastase (PDB ID: 4YM9), as presented in Fig. 2b, shows that 98.4% (239/243) of all residues are in the favored regions, 100.0% (243/243) are in the allowed regions, and 0 (0.0%) are in the disallowed regions. According to Vinsentricia *et al.* [26], a higher percentage of residues in the favored regions and a smaller percentage of nonglycine residues in the disallowed regions indicate greater stability of the protein structure. This suggests that all amino acid residues in the tyrosinase receptor (PDB ID: 6E14) and elastase receptor (PDB ID: 4YM9) can form a stable protein structural conformation that resembles the actual protein conformation and thus can be used for the validation stage of molecular docking.

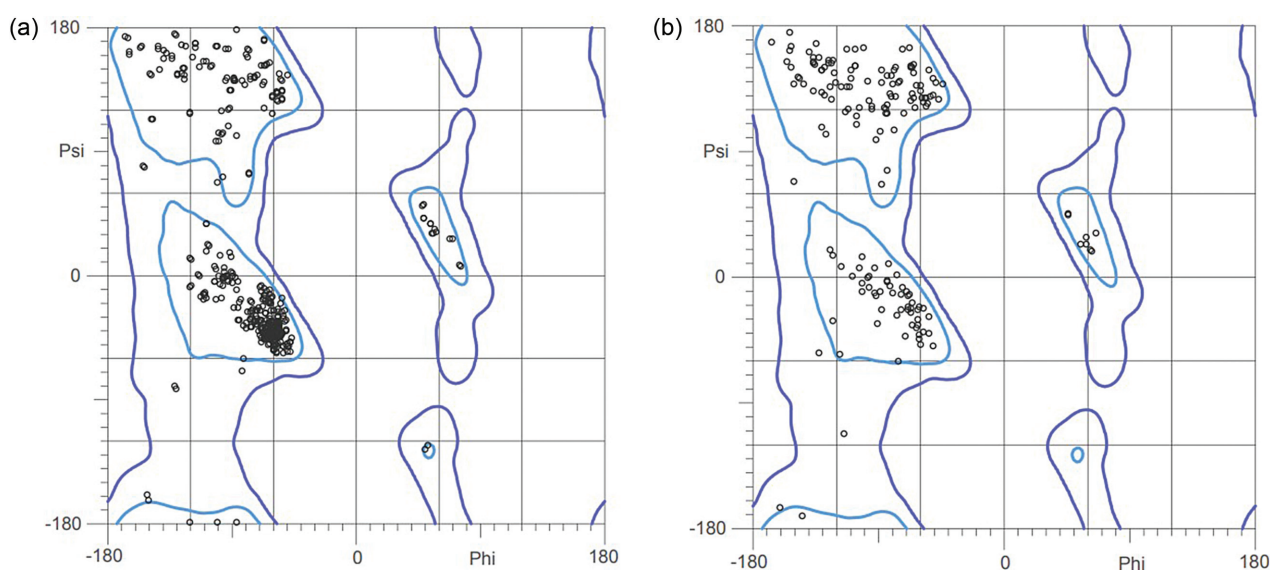
The selected receptor and its natural ligand were used for grid box validation and molecular docking. Validation for both tyrosinase and elastase enzyme

receptors showed superimposition results with an RMSD of less than 2 Å (Fig. 3). The superimposition of the natural ligand on the initial and redocking positions met the valid requirements for molecular docking simulations [27]. The redocking of the B5N natural ligand for the tyrosinase receptor showed an affinity energy value of -8 kcal/mol. In comparison, the redocking of the 4E4 natural ligand for the elastase receptor showed an affinity energy value of -4.8 kcal/mol. A more negative affinity energy indicates a stronger binding affinity [28].

Prediction of bioavailability and toxicity ligands

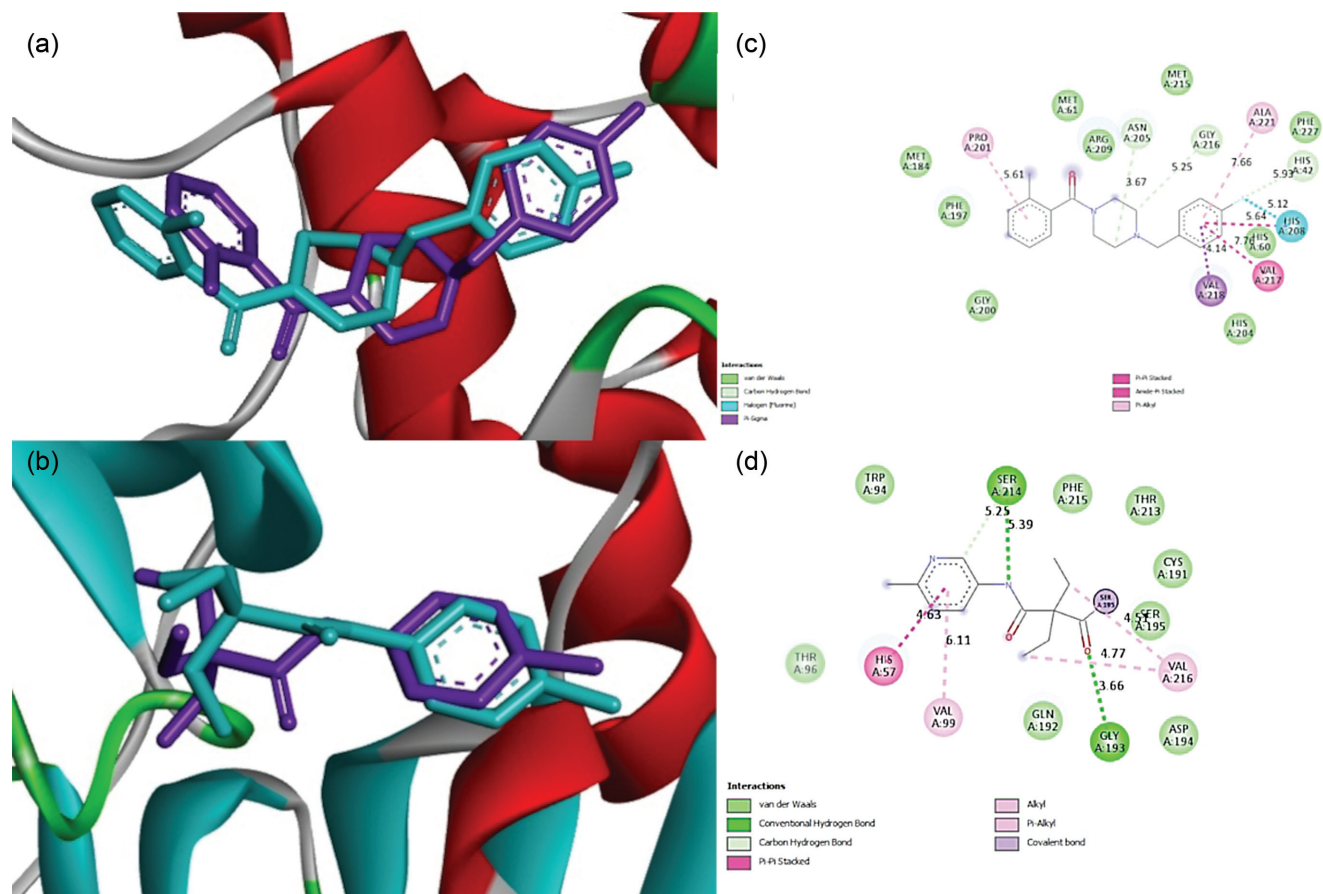
The test ligands, comprising 32 compounds identified from UPLC-MS/MS and two natural comparison ligands (B5N and 4E4), were screened for similarity with drug characteristics (bioavailability properties) using the Lipinski's rule of five (Ro5) and predicted for toxicity using admetSAR. Bioavailability measures the extent, rate, and amount of active compounds in systemic circulation that can reach the target site, making it a critical parameter for evaluating the quality and effectiveness of a drug candidate [29]. Although the bioprospecting of *H. humphreysiana* mucus is aimed at cosmeceuticals, drug-likeness and toxicity were still assessed. Drug-likeness was evaluated using Lipinski's Ro5, which predicts a compound's ability to penetrate cell layers. In cosmeceuticals, even with topical application, the ability of an active compound to penetrate the skin layer is crucial for demonstrating efficacy. Toxicity was also predicted to assess potential adverse effects if the cosmeceuticals containing the mucus are accidentally ingested during application.

Figure 2



Ramachandran plot of (a) tyrosinase receptor and (b) elastase receptor.

Figure 3



Molecular docking validation (a) Superimposition of B5N in initial (purple) and redocking (green) positions on tyrosinase (PDB ID: 6E14) with RMSD 0.767 Å; (b) superimposition of 4E4 in initial (purple) and redocking (green) positions on elastase (PDB ID: 4YM9) with RMSD 1.046 Å; (c) 2D interaction between B5N ligand and tyrosinase (PDB ID: 6E14); (d) 2D interaction between 4E4 ligand and elastase (PDB ID: 4YM9).

A compound has potentially drug-like properties if it does not violate more than two of Lipinski's rules, which are: the compound must have a molecular weight of less than or equal to 500 Da, the number of hydrogen bond donors less than or equal to 5, hydrogen bond acceptors less than or equal to 10, log P less than or equal to 5, and molar refractivity in the range of 40–130 [30,31]. Based on the study's results, 30 of the 32 tested ligands and the two comparison ligands used in this study complied with Lipinski's Ro5 rules, allowing them to proceed to ligand toxicity analysis, including skin sensitization (Table 3).

The toxicity prediction aims to identify the detrimental effects of certain compounds on humans, animals, plants, or the environment [32]. Testing drug toxicity or safety is significant in discovering and developing new drugs [33]. The virtual platform used to predict the toxicity of compounds in this study was admetSAR, with the parameters analyzed including human ether-a-go-go-related gene inhibitors, carcinogenicity, and acute oral toxicity.

The prediction results for the human ether-a-go-go-related gene inhibition show that one test ligand is categorized as a strong inhibitor ($P=0.6077$), while 29 test ligands are categorized as weak inhibitors. Based on the carcinogenicity prediction results, 21 test ligands were classified as noncarcinogenic, while nine test ligands were classified as carcinogenic, with a P value of 0.77. Based on the prediction results of acute oral toxicity in Table 3, 25 test ligands were categorized in categories III and IV, and four test ligands were in category II with a probability value. The prediction results for skin sensitization showed that among the 32 test ligands and two comparison ligands, 12 ligands might cause allergies and skin irritation due to interactions between the skin and chemical substances.

Molecular docking and visualization

The principle of molecular docking is to place the ligand into the receptor's active site, followed by evaluating the molecule based on its structural conformation and electrostatic properties [34]. This

Table 3 Analysis of Lipinski's rule and bioavailability of selected ligands from *Hemiplecta humphreysiana*

Ligand	Bioavailability analysis													
	Molecular weight (g/mol)	Log P	HD	HA	Molar refractivity	Result (*)	Human ether-a-go-go related gene (hERG) inhibition			Carcinogenicity			Acute oral toxicity	Skin sensitization
							Category	Probability	Category	Probability	Category	Probability		
B5N inhibitor	291	0.453390	0	3	71.8827995	5/5	Weak inhibitor	0.8111	Noncarcinogenic	0.9311	III	0.7284	No	
4E4 inhibitor	216	-0.422680	0	4	53.677502	4/5	Weak inhibitor	0.9962	Noncarcinogenic	0.7626	III	0.6096	Yes	
Carbonic dihydrazide, N'-[(1E)-2-chloroethylidene]-	150.5	-0.876710	4	5	32.206799	3/5	Weak inhibitor	0.9330	Carcinogenic	0.5562	III	0.5573	No	
Benzocaine	165	1.4455	2	3	46.810894	5/5	Weak inhibitor	0.9721	Carcinogenic	0.5130	III	0.7993	No	
Indoleacrylic acid	187	2.2657	2	2	54.968494	5/5	Weak inhibitor	0.9709	Noncarcinogenic	0.8816	III	0.4678	No	
7-[2-(1-adamantyl)-2-oxoethyl]-1,3-dimethyl-8-(4-methylpiperazin-1-yl)purine-2,6-dione	454	2.062201	0	8	123.44146	5/5	Weak inhibitor	0.5771	Noncarcinogenic	0.8262	III	0.7663	No	
Withanone	470	3.495399	2	6	124.511543	5/5	Weak inhibitor	0.9855	Noncarcinogenic	0.9650	I	0.4368	No	
Di(2-ethylhexyl) phthalate	390	6.433001	0	4	113.618942	4/5	Weak inhibitor	0.9063	Noncarcinogenic	0.7116	IV	0.7176	No	
Cholesteryl acetate	428	7.959503	0	2	128.599945	4/5	Weak inhibitor	0.8412	Noncarcinogenic	0.8984	III	0.8629	No	
(5E,9E,13E,17E,21E,25E)-6,10,14,18,22,26,30-Heptamethyl-5,9,13,17,21,25,29-hentriacontaneptaen-2-one	534	12.680811	0	1	177.292282	2/5	Weak inhibitor	0.6864	Carcinogenic	0.5434	III	0.8221	Yes	
Azanylidyne-[hydroxysulfamoyl(nitro)amino]methane	182	-0.836120	2	8	28.481899	3/5	Weak inhibitor	0.9376	Carcinogenic	0.500	III	0.4827	No	
(Carbonoperoxyloxydiazenyloxy) hydroxy carbonate	182	0.521	2	10	25.245598	4/5	Weak inhibitor	0.9493	Carcinogenic	0.5307	II	0.4267	No	
(2,2-Dihydroxyacetoxo)(hydroxy)acetic acid	166	-2.756700	4	7	27.960196	3/5	Weak inhibitor	0.9954	Noncarcinogenic	0.6523	III	0.4608	No	
Octylamine	129	2.3056	2	1	42.430386	5/5	Weak inhibitor	0.833	Carcinogenic	0.5244	III	0.837	Yes	
N-Butyl-N-(2-chloroethyl)-1-butanamine	191,5	2.86679	0	1	54.115986	5/5	Weak inhibitor	0.5507	Carcinogenic	0.8124	I	0.6904	Yes	
N,N-Dimethyl-4-[(E)-2-(4-pyridinyl)vinyl]aniline	224	3.317999	0	2	73.933983	5/5	Weak inhibitor	0.9437	Noncarcinogenic	0.7364	II	0.3802	No	
(-) Epinephrine	183	0.3506	4	4	48.658096	5/5	Weak inhibitor	0.7514	Noncarcinogenic	0.9322	II	0.5282	Yes	
Mirtazapine	265	2.4789	0	3	81.068985	5/5	Weak inhibitor	0.7532	Noncarcinogenic	0.9742	III	0.8137	No	

(Continued)

Table 3 (Continued)

Ligand	Bioavailability analysis													
	Lipinski analysis						Human ether-a-go-go related gene (HERG) inhibition			Carcinogenicity			Acute oral toxicity	
	Molecular weight (g/mol)	Log P	HD	HA	Molar refractivity	Result (*)	Category	Probability	Category	Probability	Category	Probability	Category	Probability
(2E)-2-(Mesitylmethylene)-N-(3-methylphenyl)hydrazinecarbothioamide	311	4.008079	2	3	97.849388	5/5	Weak inhibitor	0.8821	Carcinogenic	0.5778	III	0.5878	No	
2,2'-(Tridecylimino)diethanol	287	3.583999	2	3	87.072563	5/5	Weak inhibitor	0.5359	Noncarcinogenic	0.5477	III	0.8822	Yes	
Perazine	339	4.055698	0	2	104.688965	5/5	Weak inhibitor	0.8613	Noncarcinogenic	0.9625	II	0.6788	No	
2-Amino-6-benzyl-3-cyano-4,5,6,7-tetrahydrothieno[2,3-c]pyridine	269	2.52758	2	3	76.773399	5/5	Weak inhibitor	0.7668	Noncarcinogenic	0.9467	II	0.4997	No	
Phenyl(2-pyridinyl)methanone	183	2.3126	0	2	54.111488	5/5	Weak inhibitor	0.9491	Noncarcinogenic	0.9102	III	0.7042	Yes	
2-N-[2-(methylamino)-3-[2-(methylamino)ethylamino]propyl]-3-N-[2-(methylideneamino)ethyl]propane-1,2,3-triamine	287	-2.409499	7	7	87.774887	3/5	Weak inhibitor	0.9226	Noncarcinogenic	0.7019	III	0.7255	Yes	
2-[(4-Cyclohexyl-5-[1-(dimethylamino)propyl]-4H-1,2,4-triazol-3-yl)sulfanyl]-1-(4-morpholinyl)ethanone	395	2.7469	0	6	106.98597	5/5	Weak inhibitor	0.8925	Noncarcinogenic	0.7284	III	0.4823	No	
1-hexadecyl-2-amino-2-deoxy-sn-glycerol	315	4.803899	3	3	96.192162	5/5	Weak inhibitor	0.8176	Noncarcinogenic	0.7837	III	0.6449	Yes	
1-[1-[(4S)-7-(diaminomethylideneamino)-4-[4-(diaminomethylideneamino)butylamino]heptyl]-2-oxopyrimidin-4-yl]-3-methylurea	451	-0.891198	11	13	127.114662	2/5	Weak inhibitor	0.6383	Noncarcinogenic	0.9240	III	0.6615	No	
Dibutyl phthalate	278	3.600399	0	4	76.822975	5/5	Weak inhibitor	0.9412	Noncarcinogenic	0.7325	IV	0.6453	No	
Benzenemethanamine	273	4.893399	0	1	89.212975	5/5	Weak inhibitor	0.7882	Carcinogenic	0.5816	III	0.7236	Yes	
4,4'-Bis(1-phenylethyl)diphenylamine	377	7.733804	1	1	124.084671	4/5	Weak inhibitor	0.9397	Carcinogenic	0.5318	III	0.9318	No	
Alverine	281	4.5739	0	1	91.639969	5/5	Strong inhibitor	0.6077	Noncarcinogenic	0.6473	III	0.5123	Yes	
N,N-Dimethylsphingosine	327	4.527099	2	3	100.785561	5/5	Weak inhibitor	0.8257	Noncarcinogenic	0.6686	III	0.6504	Yes	
N,4-Bis(1-phenylethyl)-N-[4-(1-phenylethyl)phenyl]aniline	481	9.889506	0	1	157.798172	3/5	Weak inhibitor	0.9445	Carcinogenic	0.7241	III	0.8816	No	
2-Sulfanylfuro[3,4-d]pyrimidine-5,7-dione	182	0.0759	0	5	39.029999	4/5	Weak inhibitor	0.9824	Noncarcinogenic	0.9450	III	0.6021	No	

aligns with the concept of competitive inhibition, which explains that molecules other than substrates compete for binding to the active site of the enzyme. Therefore, it is essential to analyze the percentage of the inhibition coverage area on the receptor's active site [35]. Competitive inhibition occurs because the inhibitor has a structure that resembles the substrate, allowing the inhibitor to compete for binding to receptors or enzymes [36]. The comparison ligands (B5N and 4E4) and the 30 test ligands passed bioavailability and toxicity predictions. The results show that the B5N ligand has a binding affinity energy value of -8 kcal/mol with an inhibition coverage area of 55.55% on the active site of the tyrosinase receptor (Table 4). The 4E4 ligand has a binding affinity energy value of -4.8 kcal/mol with an inhibition coverage area of 100% on the active site of the elastase receptor (Table 5). The molecular docking results were visualized in two dimensions using Discovery Studio to observe the interaction between the ligand and receptors.

The visualization results show hydrogen bonds, hydrophobic interactions, van der Waals bonds, and the interacting receptor amino acid residues. A hydrophobic bond between the ligand and the protein is essential to stabilize the conformation of the ligand on the protein binding site [37]. Meanwhile, van der Waals interactions function as stabilizers for the complex, so the greater the number of van der Waals interactions between the ligand and receptors, the more stable the formed bonds [38]. The interactions between the ligand and the tyrosinase receptor are shown in Table 4, while the interactions between the ligand and the elastase receptor are shown in Table 5. The interaction of the B5N inhibitor with the tyrosinase receptor forms five hydrophobic interactions, seven van der Waals interactions, and two hydrogen bonds. The hydrogen-bonded amino acid residues are Asn205 with bond distances of 4.08 and 5.02 Å and Arg209 with a bond distance of 4.22 Å (Fig. 3a, c). The interaction of the 4E4 inhibitor with the elastase receptor forms three hydrophobic interactions, eight van der Waals interactions, and two hydrogen bonds. The hydrogen-bonded amino acid residues are Ser214 with bond distances of 5.25 and 5.39 Å and Gly193 with a bond distance of 3.66 Å (Fig. 3b, d). Hydrogen bonds with a distance in the range of 2.2–2.5 Å are categorized as strong interactions, distances of 2.5–3.2 Å are categorized as moderate interactions, and distances in the range of 3.2–4.0 Å are categorized as weak interactions [39]. This indicates that the B5N and 4E4 inhibitors both have hydrogen bonds with the

amino acid residues on the active sites of the tyrosinase and elastase receptors. However, these interactions are categorized as weak.

The score, based on the accumulation of the affinity energy value and the percentage of the inhibition coverage area for the tested ligands, determines the number of compounds with the potential to inhibit tyrosinase and elastase enzymes. The scoring results showed that 13 ligands have a higher scoring value than the B5N inhibitor (Fig. 4). The ligands with potential as tyrosinase inhibitors are benzocaine, indole acrylic acid, 7-[2-(1-adamantyl)-2-oxoethyl]-1,3-dimethyl-8-(4-methylpiperazin-1-yl) purine-2,6-dione, withanone, N, N-dimethyl-4-[(E)-2-(4-pyridinyl vinyl)aniline, (2E)-2-(mesitylmethylene)-N-(3-methylphenyl)hydrazinecarbothioamide, perazine, 2-amino-6-benzyl-3-cyano-4,5,6,7-tetrahydrothieno [2,3-c]pyridine, phenyl(2-pyridinyl)methanone, 1-[1-(4S)-7-(diaminomethylideneamino)-4-[4-(diaminomethylideneamino)-butylamino]heptyl]-2-oxopyrimidin-4-yl]-3-methylurea, benzenemethanamine, 4,4'-bis(1-phenylethyl) diphenylamine, and alverine. In addition, there are 12 ligands with higher scoring values than the 4E4 inhibitor and thus are potential catalase inhibitors (Fig. 5). The ligands are indoleacrylic acid, 7-[2-(1-adamantyl)-2-oxoethyl]-1,3-dimethyl-8-(4-methylpiperazin-1-yl) purine-2,6-dione, withanone, cholesteryl acetate, mirtazapine, (2E)-2-(mesitylmethylene)-N-(3-methylphenyl) hydrazinecarbothioamide, perazine, 2-amino-6-benzyl-3-cyano-4,5,6,7-tetrahydrothieno[2,3-c] pyridine, 2-({4-cyclohexyl-5-[1-(dimethylamino)-propyl]-4H-1,2,4-triazol-3-yl}sulfanyl)-1-(4-morpholinyl)-ethenone, 1-[1-(4S)-7-(diaminomethylideneamino)-4-[4-(diaminomethylideneamino)-butylamino]heptyl]-2-oxopyrimidin-4-yl]-3-methylurea, benzenemethanamine, and 4,4'-bis(1-phenylethyl) diphenylamine.

Indoleacrylic acid (95.62%) has the highest scoring value based on the molecular docking of the test ligands to the tyrosinase receptor, followed by 4,4'-bis(1-phenylmethyl)diphenylamine (94.51%) and withanone (93.26%). Except for 4,4'-bis(1-phenylmethyl)diphenylamine, these compounds are the most promising candidates for anti-tyrosinase activity. Withanone (134.37%) also achieved the highest scoring value in the molecular binding of the test ligands to the elastase receptor, followed by 4,4'-bis(1-phenylethyl)diphenylamine (133.33%) and 7-[2-(1-adamantyl)-2-oxoethyl]-1,3-dimethyl-8-(4-

Table 4 Types of interactions between ligands and amino acid residues in tyrosinase receptor

Ligand	Amino acid residues					Scoring (%)
	Affinity energy (kcal/mol)	Hydrogen bonds (distance in nm)	Hydrophobic interaction (distance in nm)	Van der Waals	Percentage of binding area coverage on the active site (%)	
B5N inhibitor	-8	Asn205 (4.08; 5.02), Arg209 (4.22)	Ala221 (7.12), Val218 (4.25), His208 (5.09), Arg209 (4.36; 5.22), Pro201 (5.32)	Phe227, His204, Gly196, Gly200, Phe197, Gly216, Val217	55.55	77.77
Carbonic dihydrazide, N'-[(1E)-2-chloroethylidene]-	-5.1	His42 (6.31)	His208 (5.42), Phe197 (6.54)	Asn205, Phe227, Gly216, Val217, Ala221, Phe65, Met215, Val218, His60, His204, Met61	55.55	59.65
Benzocaine	-7.2	His60 (5.44), Arg209 (4.73)	Val218 (3.75), His208 (4.15), Phe197 (5.79)	Gly216, Val217, Ala221, Met215, Phe227, His42, His204, Asn205, Pro201	77.78	83.89
Indoleacrylic acid	-7.3	His42 (5.18), His60 (5.56)	Val218 (5.53)	His69, His231, His208, Asn205, Phe65, Arg209, Pro201, Phe197, Met61, His204, Ala221, Phe227	100	95.62
7-[2-(1-adamantyl)-2-oxoethyl]-1,3-dimethyl-8-(4-methylpiperazin-1-yl) purine-2,6-dione	-8	Arg209 (4.38), Glu195 (5.66), His204 (6.14)	His208 (4.37; 5.63), Val218 (4.64; 5.57), Val217 (6.21), Phe197 (5.37)	Met184, Met61, Pro201, Asn205, His60, His42, Ala221, Met215, Gly216	66.67	83.33
Withanone	-8.7	-	His208 (5.02), His60 (4.35), His204 (6.13)	Met184, Met61, Val218, Val217, Gly216, Ala221, Met215, His42, Phe227, Arg209, Pro201, Phe197, Asn205, Gly200	77.78	93.26
Di(2-ethylhexyl) phthalate	-5.6	-	Val218 (4.36), Pro201 (7.80), Phe197 (6.09), Val217 (5.09), His208 (4.95), His204 (7.10)	His60, Met61, Asn205, Gly200, Arg209, Pro219, Gly216, Ala221, His42	77.78	73.89
Cholesteryl acetate	-7.2	-	His208 (4.70), Phe197 (5.34; 6.21), Arg209 (5.44)	Gly200, Glu158, Pro201, Asn205, Val217, Gly216, Met215, Ala221, Val218, His204, Met61, Met184	55.55	72.77
Azanylidyne-[hydroxysulfamoyl(nitro) amino]methane	-5.5	Met215 (5.34), Asn205 (3.83), His60 (4.40), His208 (3.82; 4.61), His204 (5.21)	-	Val217, Ala221, His231, His42, Phe227, Phe197, Glu195, Met61, Val218, Gly216	66.67	67.71
(Carbonoperoxyloxydiazanylyl) hydroxy carbonate	-5.4	Gln248 (5.49), His245 (6.29), Arg246 (3.78; 3.18; 4.68), Gln242 (3.48; 4.56), Trp238 (5.21), Tyr177 (3.65)	-	Asn247, Asn278, Met277, Asn249, Tyr250, Trp241	0	33.75
(2,2-Dihydroxyacetoxyl)(hydroxy)acetic acid	-5.1	Glu195 (4.38), His204 (5.83; 5.82)	-	Asn205, Val218, His208, Met215, Val217, Ala221, Gly216, His42, Phe227, His60, Phe197, Met61	55.55	59.65
Octylamine	-4.4	Glu195 (3.73), Asn205 (4.18), His60 (4.44)	His208 (4.16; 5.09), Val218 (3.88; 4.75), Ala221 (5.79)	His42, Phe227, Met61, Phe197, His204	55.55	55.27
N,N-Dimethyl-4-[(E)-2-(4-pyridinyl)vinyl] aniline	-7.4	His60 (5.71), Met215 (6.01)	Val218 (4.18), His208 (5.22), Ala221 (5.86), Phe197 (5.26; 5.76), Pro201 (3.99)	Val217, Phe227, His42, His204, Asn205, Arg209, Gly200	77.78	85.14
(-) Epinephrine	-6.2	Met215 (4.50), Arg209 (4.59)	Val218 (4.54), His208 (5.30)	Pro201, Asn205, Phe197, Met61, Gly216, Val217, Ala221, Phe227, His42, Pro222, His60, His204	77.78	77.64

(Continued)

Table 4 (Continued)

Ligand	Amino acid residues					Scoring (%)
	Affinity energy (kcal/mol)	Hydrogen bonds (distance in nm)	Hydrophobic interaction (distance in nm)	Van der Waals	Percentage of binding area coverage on the active site (%)	
Mirtazapine (2E)-2-(Mesitylmethylene)-N-(3-methylphenyl)hydrazinecarbothioamide	-6.7 -7.7	Gly216 (5.60) Asn205 (3.12)	Arg209 (5.87), Pro201 (4.07), Val218 (6.38) Val218 (3.86; 4.02), His208 (4.05; 5.17), Phe197 (5.93; 6.38), His60 (6.41), His42 (6.03), Phe227 (6.29), Ala221 (4.84; 4.89), Pro201 (6.08; 4.70)	Asn205, His208, Gly216 Met215, Val217, Gly216, Glu195, Arg209, Gly200, Met61, His204	44.44 66.67	64.09 81.46
2,2'-(Tridecylimino)diethanol	-5	Asn205 (4.23)	Pro201 (4.23), Phe197 (4.97; 7.95), Val218 (4.56)	Gly200, Arg209, Met61, His60, His204, Phe227, Phe65, His231, His69, His42, His208, Gly216, Val217, Met184	77.78	70.14
Perazine	-6.9	His60 (6.01), Asn205 (4.63)	Arg209 (7.38), His208 (4.03; 5.27), Phe197 (5.60), Pro201 (6.14)	Gly216, Val217, Met215, Val218, Ala221, His42, -Phe227, His204, Met184, Gly196, Gly200	77.78	82.01
2-Amino-6-benzyl-3-cyano-4,5,6,7-tetrahydrothieno[2,3-c]pyridine	-7.8	Gly216 (4.41)	Val218 (3.87), Phe197 (7.03), His208 (4.33), Ala221 (6.11)	His42, Phe227, Met215, Val217, Met61, Met184, Gly200, Gly196, Pro201, Asn205, Arg209, His204, His60	77.78	87.64
Phenyl(2-pyridinyl)methanone	-7.1	-	Val218 (4.32), His208 (5.08), Ala221 (7.36)	His60, His42, Phe227, Met215, Val217, Gly216, Arg209, Met61, Phe197, Asn205, His204, Pro201	77.78	83.32
2-N-[2-(methylamino)-3-[2-(methylamino)ethylamino]propyl]-3-N-[2-(methylideneamino)ethyl]propane-1,2,3-triamine	-4	Asn205 (3.65), Met215 (5.82), Val218 (3.09)	His208 (3.96)	Ala221, His60, His42, Met61, Arg209, Phe197, Pro201, Gly200, Gly216, Val217, His204	77.78	63.89
2-[(4-Cyclohexyl-5-[1-(dimethylamino)propyl]-4H-1,2,4-triazol-3-yl)sulfanyl]-1-(4-morpholinyl)ethanone	-6.4	Asn205 (4.21), Phe197 (4.69), His60 (4.70)	Pro201 (4.76)	Met184, His204, Val218, Met61, His208, Arg209, Gly196, Gly200	66.67	73.33
1-hexadecyl-2-amino-2-deoxy-sn-glycerol	-4.4	Gly200 (4.08)	His204 (6.71), His60 (5.42), Val128 (3.69; 5.16), His208 (5.48; 4.05), Pro201 (4.26; 7.15), Phe197 (4.55; 5.69)	Glu158, Val217, Met215, Ala221, His42, Phe227, Met61, Asn205, Gly196, Arg209	77.78	66.39
1-[1-(4S)-7-(diaminomethylideneamino)-4-[4-(diaminomethylideneamino)butylamino]heptyl]-2-oxopyrimidin-4-yl]-3-methylurea	-6	Glu195 (4.90), Asn205 (3.08), His42 (5.57), His231 (5.86), His204 (6.17), Gly46 (5.10)	Val218 (4.93)	Met61, Asn57, Arg209, Pro201, Gly216, Pro219, Val217, His49, Lys47, Ala221, Pro222, Phe227, His69, Phe65, Phe197, His60, His208	100	87.5
Dibutyl phthalate	-5.8	His204 (5.80), His60 (4.74), Asn205 (4.71)	Val218 (3.88), His208 (4.54), Val217 (6.15), His204 (7.08), Ala221 (6.47), Met61 (5.47), Pro201 (4.37), Phe197 (5.43)	His42, Phe227, Met215, Arg209, Gly216	77.78	75.14
Benzenemethanamine	-7.2	Gly216 (5.16), Asn205 (3.77; 3.83)	Val218 (4.17), His208 (4.56), Ala221 (6.87), Pro201 (5.96)	His204, His60, His42, Phe227, Met215, Phe197, Val217, Arg209	77.78	83.89
4,4'-Bis(1-phenylethyl)diphenylamine	-8.9	-	-	Met61, His204, Val218, Met61, His208, Arg209, Gly196, Gly200	77.78	94.51 (Continued)

Table 4 (Continued)

Ligand	Amino acid residues					Scoring (%)
	Affinity energy (kcal/mol)	Hydrogen bonds (distance in nm)	Hydrophobic interaction (distance in nm)	Van der Waals	Percentage of binding area coverage on the active site (%)	
Alverine	-6.9	-	Val218 (5.22), His208 (5.22), Val217 (7.56), Ala221 (5.65), Pro201 (4.30)	Phe227, His42, His204, His60, Phe197, Met61, Met184, Gly200, Asn199, Arg209, Asn205, Met215	77.78	82.01
N,N-Dimethylsphingosine	-4.3	-	Val218 (4.39), His208 (4.24), Gly200 (3.99), Ala221 (6.76), Pro201 (4.19)	Met215, Phe227, Val217, His42, His60, His204, Met61, Asn205, Arg209, Phe197, Gly196	55.55	54.65
2-Sulfanylfuro[3,4-d]pyrimidine-5,7-dione	-6.4	-	Met61 (5.39), Phe197 (6.69), Val218 (5.16; 3.66; 6.90), His60 (6.50), His204 (6.78), His208 (4.70; 4.56)	Pro201, Glu158, Met184, Gly200, Asn205, Val217, Gly216	44.44	62.22
			His208 (6.25; 4.75), Val217 (6.52), Ala221 (6.76)	Met61, Phe197, Asn205, His204, His60, Phe227, His42, Gly216, Met215		

methylpiperazin-1-yl)purine-2,6-dione (129.16%). These compounds are the most promising candidates for elastase enzyme inhibition, except for 4,4'-bis(1-phenylmethyl)diphenylamine. The latter is considered carcinogenic based on the admetSAR analysis, with category III acute oral toxicity, and thus is not a viable candidate for anti-tyrosinase and anti-elastase activities. Although indoleacrylic acid and withanone have the highest scoring values, they are not classified as the compounds with the highest abundance in the mucus of *H. humphreysiana* Lea, 1840.

The mucus of land snails primarily consists of allantoin, glycolic acid, collagen, and elastin [5]. Moreover, mucus from certain land snail species often contains mucin, achacin, and mitomycin. However, our study found that the mucus of *H. humphreysiana* does not contain allantoin (C₄H₆N₄O₃) or mitomycin (C₁₅H₁₈N₄O₅). Glycolic acid (alpha-hydroxyacetic acid) can penetrate the skin, increase collagen synthesis by fibroblasts, and modulate matrix degradation and collagen synthesis through cytokines released by keratinocytes. This process accelerates epidermal turnover, prevents melanin formation, directly inhibits tyrosinase activity, and enhances UV-induced pigmentation [40]. We detected a similar compound in the mucus of *H. humphreysiana*, namely (2,2-dihydroxyacetoxy) (hydroxy) acetic acid (C₄H₆O₇).

Each species of land snail seems to have distinct glycoproteins involved in antimicrobial activity. Hemocyanin β c-HaH is an antimicrobial peptide isolated from the mucus of *H. aspersa* [5]. In contrast, achacin was identified in the 30 and 60 kDa protein bands of *L. fulica* found in Thailand [15]. This glycoprotein demonstrated antimicrobial activity against *Escherichia coli* and *Staphylococcus aureus* [41]. The protein band of *H. distincta* from Thailand differs from achacin, suggesting the need for further investigation into its antimicrobial molecules [15].

The mucus from *L. fulica*, a well-known invasive alien land snail species, contains various bioactive compounds. One of the identified bioactive compounds from this species is alkaloids [42]. Alkaloids contain at least one nitrogen atom in a heterocyclic ring structure and possess antimicrobial and antioxidant properties [43,44]. They also have anti-inflammatory activity, which makes them potential candidates for drug formulations to treat inflammation in the body [45].

The UPLC-MS/MS QTOF analysis with methanol and DCM solvents detected 33 bioactive compounds in the mucus of *H. humphreysiana*. Among these, 14 alkaloids were identified (seven suspected and seven confirmed). The confirmed alkaloids are benzocaine (C₉H₁₁NO₂), benzenemethanamine (C₂₀H₁₁N), (-) epinephrine (C₉H₁₃NO₃), mirtazapine (C₁₇H₁₉N₃), perazine (C₂₀H₂₅N₃S), phenyl(2-pyridinyl) methanone (C₁₂H₉NO), and indoleacrylic acid (C₁₁H₉NO₂).

Indoleacrylic acid is the most potential candidate for anti-tyrosinase activity. Tyrosinase is a metalloenzyme found in many microorganisms, animals, plants, and humans, which plays a role in the biosynthesis of melanin [46,47]. Anti-tyrosinase activity can inhibit the melanogenesis mechanism, thereby preventing melanin hyperpigmentation. Consequently, it can brighten the skin by reducing the effect of skin darkening. Indoleacrylic acid in the mucus of *H. humphreysiana* is the most potential candidate for anti-tyrosinase. Furthermore, indoleacrylic acid (IA) is confirmed to have an anti-inflammatory response and enrich antioxidant pathways, making it relevant for human peripheral blood mononuclear cells [48].

The mucus of *H. humphreysiana* is proven to contain bioactive compounds that can inhibit elastase. Elastase is a proteolytic enzyme that breaks down elastin, collagen, fibronectin, and other extracellular matrix proteins [49]. Elastase plays a role in degrading elastin in the skin. Elastin is an extracellular matrix protein of connective tissue that provides elasticity to the skin, lungs, blood vessels, and ligaments. It contains more than 30% glycine, and about 75% of its entire sequence consists of only four hydrophobic amino acids (glycine, valine, alanine, and proline). Elastin supports the structure and physical properties of the skin [50]. It forms elastic fibers in the dermis of the skin, influencing skin elasticity. Damage to elastin fibers leads to decreased skin elasticity [12]. The secretion and activation of elastase from skin fibroblasts in response to UV irradiation and cytokines released by keratinocytes are responsible for the degeneration of the three-dimensional structure of elastic fibers during wrinkle formation [13].

Withanone (C₂₈H₃₈O₆) is a glycerophospholipid found in the mucus of *H. humphreysiana*, which has the highest binding score for elastase inhibitors. The compound is a natural product from plants of the Solanaceae family, including potatoes, tomatoes, and

peppers, as well as Ashwagandha or Indian ginseng. This is the first record of withanone being isolated from animals. The compound is also a potential candidate for cancer therapy [51]. The study by Noothuan *et al.* [15] showed that the mucus of *L. fulica* and *H. distincta* contains anti-tyrosinase and antioxidant activities, which can benefit therapeutic and cosmetic applications. Various metabolites in *H. humphreysiana* mucus have been identified and may have bioactivities. However, the present study was limited to anti-tyrosinase and anti-elastase activities, which were confirmed by molecular docking studies. These findings support the potential of *H. humphreysiana* mucus as a whitening agent and anti-wrinkle candidate.

Conclusion

To uncover the significant potential of a species, bioprospecting and identifying its bioactive compounds are essential. This study initiates the bioprospecting of *H. humphreysiana* mucus as nutraceuticals for future research. The metabolomic study using UPLC-MS/MS QTOF identified 33 bioactive compounds from *H. humphreysiana* mucus. Molecular docking studies indicate that indoleacrylic acid and withanone are lead compounds for anti-tyrosinase activity, while withanone and 7-[2-(1-adamantyl)-2-oxoethyl]-1,3-dimethyl-8-(4-methylpiperazin-1-yl) purine-2,6-dione are lead compounds for anti-elastase activity. The presence of these lead compounds in *H. humphreysiana* mucus suggests potential applications as a whitening and an anti-wrinkle agent, respectively.

Acknowledgments

The authors acknowledge the government of the Republic of Indonesia for supporting this research through funding from the Deputy for Life Sciences, Indonesian Institute of Sciences (LIPI).

Funding: This research was fully supported by the government of the Republic of Indonesia through the Deputy for Life Sciences, Indonesian Institute of Sciences (LIPI), budget implementation list year 2021 number: 45/A/DH/2021.

Authors' contributions: U.M.S.P., P.R.F., R.R.E., and L.A. contributed to the concept, design, and implementation of the research as well as the preparation and review of the manuscript. P.P., A.S. N., and I.G. contributed to experimental studies, literature search, and data analysis.

Table 5 Types of interactions between ligands and amino acid residues in elastase receptor

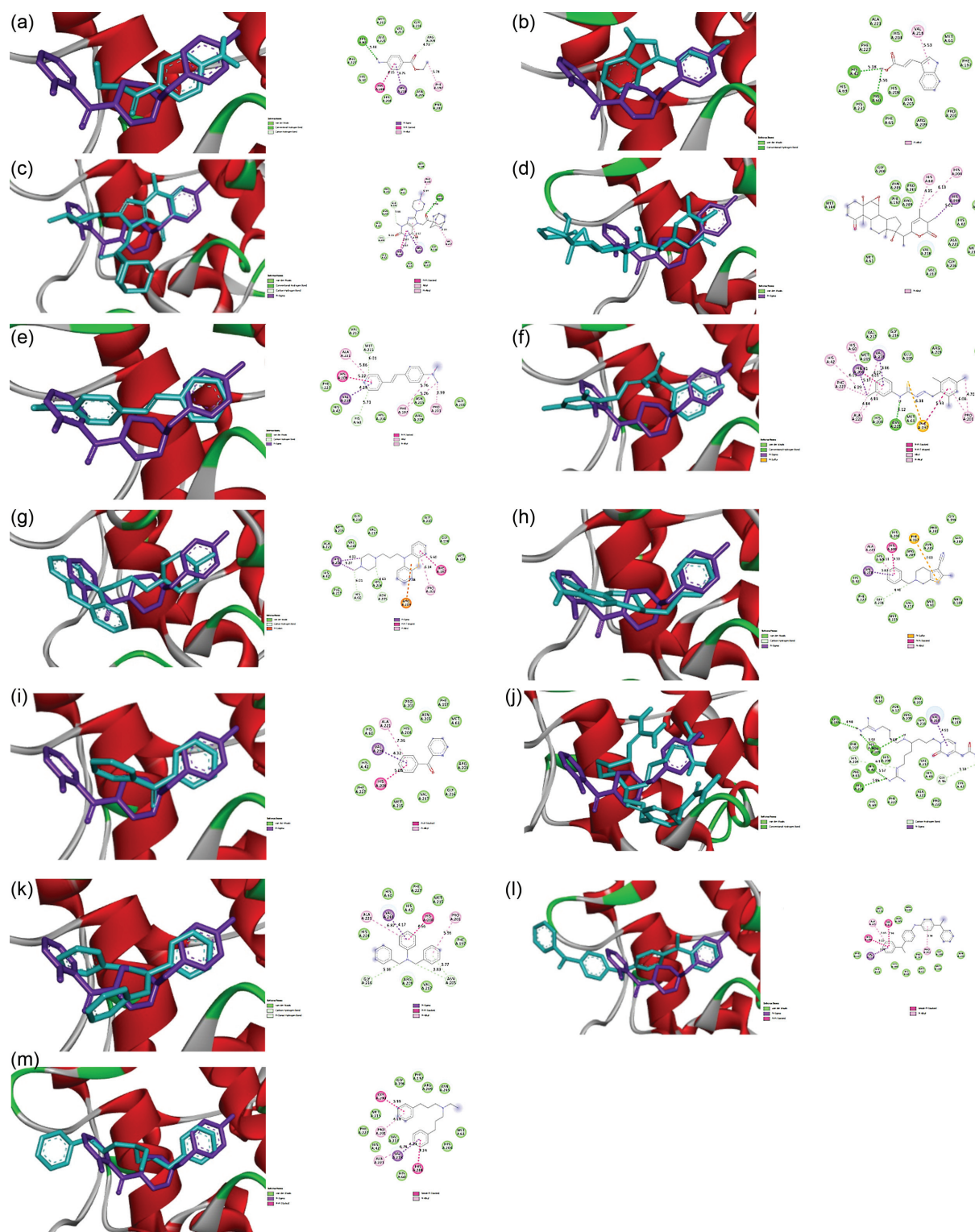
Ligand	Amino acid residues					Percentage of binding area coverage on the active site (%)	Scoring (%)
	Affinity energy (kcal/mol)	Hydrogen bonds (distances)	Hydrophobic interaction (distances)	Van der Waals			
4E4 inhibitor	-4.8	Ser214 (5.25; 5.39), Gly193 (3.66)	His57 (4.63), Val99 (6.11), Val216 (4.77; 4.51)	Trp94, Phe215, Thr213, Cys191, Ser195, Asp194, Gln192, Thr96	100	100	
Carbonic dihydrazide, N'-[(1E)-2-chloroethylidene]-	-3.9	Ser195 (2.92; 3.67), Ser214 (6.11)	His57 (6.38), Asp194 (3.67)	Phe215, Val216, Thr226, Thr213, Gly190, Cys191, Gly193, Gln192	100	90.62	
Benzocaine	-5	Val216 (4.63), Ser195 (5.03)	Val216 (4.38; 4.38)	Arg217A, Ser217, Phe215, Cys215, Gly190, Asp194, Thr226, Thr213, Gln192	25	64.58	
Indoleacrylic acid	-5.8	Ser195 (3.77), Val216 (5.12; 5.65)	His57 (6.51), Val99 (6.39)	Arg217A, Phe215, Gln192, Gly193, Cys191, Asp194, Thr213, Gly190, Ser214	100	110.41	
7-[2-(1-adamantyl)-2-oxoethyl]-1,3-dimethyl-8-(4-methylpiperazin-1-yl)purine-2,6-dione	-7.6	Ser195 (4.28), Asp60 (5.18), His57 (4.74)	Val216 (4.13; 5.92)	Arg61, Thr41, Leu150, Gly193, Leu143, Gln192, Phe215, Ser214	100	129.16	
Withanone	-8.1	Ser214 (4.87), His57 (4.50)	His57 (4.60)	Ser195, Gln192, Gly193, Cys42, Thr41, Tyr35, Leu63, Arg61, Asp60, Thr96, Trp94, Val99, Phe215	100	134.37	
Di(2-ethylhexyl) phthalate	-4.5	Ser195 (5.10), His57 (4.23), Phe215 (5.71)	His57 (5.99), Val99 (4.64), Phe215 (5.23; 6.03), Arg217A (7.66), Trp171 (6.30)	Trp94, Ser214, Thr174, Val216, Gln192, Ser217	75	84.37	
Cholesteryl acetate	-7.3	Ser195 (4.91)	His57 (4.64), Val99 (4.70; 5.19), Arg217A (6.59)	Thr174, Trp171, Ala99A, Phe215, Val216, Gln192, Cys191, Ser214, Thr213, Thr96, Asp97	75	113.54	
Azanylidene-[hydroxysulfamoyl(nitro)amino] methane	-5.2	Tyr164 (5.32), Arg230 (5.00), Ile129 (3.77)	-	Cys167, Val162, Val180, Leu130, Thr161, Ala131, Asn132, Asp163, Met179, Asn177	0	54.165	
(Carbonperoxyloxydiazenyl) hydroxy carbonate	-3.9	Ser195 (4.81), Phe215 (5.54)	-	Val216, Cys191, Gly190, Thr213, Ser214, His57, Arg217A, Gln192, Ser217	75	78.12	
(2,2-Dihydroxyacetoxy)(hydroxy)acetic acid	-4.9	Ser195 (3.36; 3.81; 4.98), Cys191 (3.91), Phe215 (5.70)	-	His57, Thr226, Gly190, Val216, Thr213, Asp194, Gly193, Gln192	75	88.54	
Octylamine	-5.1	Asn177 (2.93)	Arg230 (5.14), Ile129 (5.11), His210 (4.62), Leu130 (3.77; 3.91), Val180 (4.16; 4.26; 5.01)	Tyr164, Met179, Cys181, Asp163, Val162, Thr161, Thr128	0	53.12	
N,N-Dimethyl-4-[(E)-2-(4-pyridinyl)vinyl] aniline	-4.4	Thr174 (5.03)	Trp171 (6.98), Phe215 (4.98), Val99 (4.93), Arg217A (5.66)	Ser214, Ala99A, Val216, Ser217	25	58.33	
(-) Epinephrine	-5	Asp60 (5.65), Thr96 (3.11; 4.79), Ser214 (4.16), Ser195 (4.06)	His57 (4.38)	Val216, Phe215, Val99, Trp94	75	89.58	
Mirtazapine	-6.6	Val216 (5.55)	His57 (4.92), Val216 (4.85), Val99 (4.84)	Ser195, Ser214, Trp94, thr96, Arg217A, Phe215	75	106.25	
(2E)-2-(Mesitylmethylene)-N-(3-methylphenyl)hydrazinecarbothioamide	-6.2	Ser214 (4.33), Val216 (3.38)	Val99 (4.11; 5.30; 5.57; 6.38), His57 (4.37; 4.39), Trp94 (6.99)	Gln192, Trp171, Arg217A, Phe215, Ser195	75	102.08	
2,2'-(Tridecylimino)diethanol	-4.6	Ser195 (3.34; 3.57; 4.85), Cys191 (3.94), Ser214 (5.61)	Arg217A (5.68), Trp171 (6.79), Phe215 (4.75; 6.43), Val99 (4.46; 5.14; 5.39)	Thr174, Ala99A, Val216, His57, Gly193, Thr213, Gln192, Asp194, Gly190	100	97.91	

(Continued)

Table 5 (Continued)

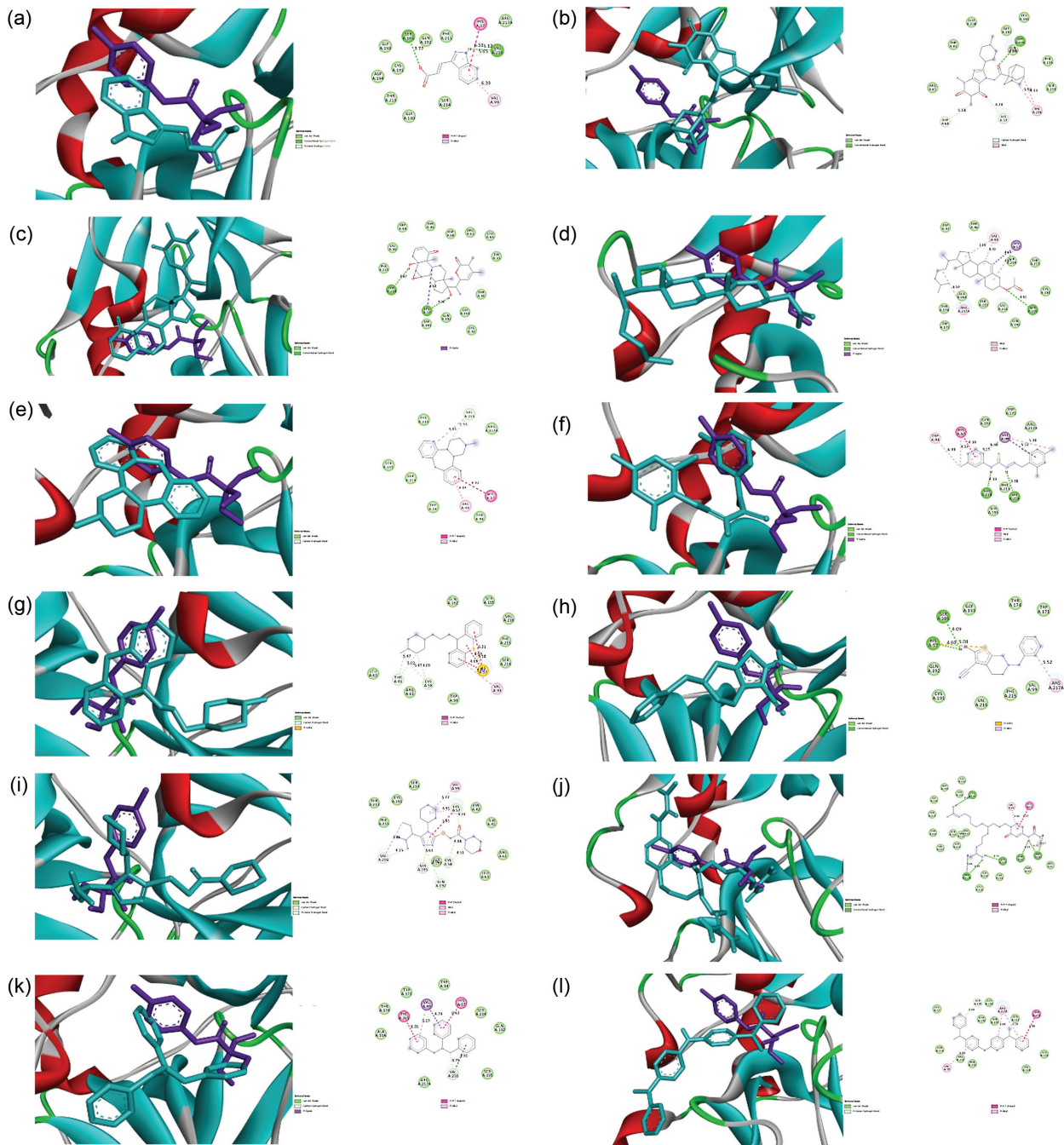
Ligand	Amino acid residues					Scoring (%)
	Affinity energy (kcal/mol)	Hydrogen bonds (distances)	Hydrophobic interaction (distances)	Van der Waals	Percentage of binding area coverage on the active site (%)	
Perazine	-6.4	Thr41 (5.02; 5.47), Cys58 (4.09; 5.47)	His57 (4.69; 4.69; 5.58; 6.21), Val99 (5.66)	Leu63, Arg61, Trp94, Gln192, Ser195, Val216, Phe215, Ser214	75	104.16
2-Amino-6-benzyl-3-cyano-4,5,6,7-tetrahydrothieno[2,3-c]pyridine	-6.2	His57 (4.60), Ser195 (4.09)	His57 (5.08), Arg217A (5.52)	Gln192, Cys191, Val216, Phe215, Val99, Trp171, Thr174, Gly193	75	102.08
Phenyl(2-pyridinyl)methanone	-5.1	-	Val99 (4.61; 5.07), His57 (5.79)	Ser214, Thr96, Trp94, Phe215, Val216, Trp171, Arg217A	50	78.12
2-N-[2-(methylamino)-3-[2-(methylamino)ethylamino]propyl]-3-N-[2-(methylideneamino)ethyl]propane-1,2,3-triamine	-4.5	Ser195 (4.72), Val216 (3.24; 3.59), Thr96 (4.93)	-	Arg217A, Ser217, Ser214, Trp94, Val99, Phe215, His57, Gln192, Thr213, Gly193, Thr41, Cys58, Cys42	100	96.87
2-[(4-Cyclohexyl-5-[1-(dimethylamino)propyl]-4H-1,2,4-triazol-3-yl)sulfanyl]-1-(4-morpholinyl)ethanone	-6.6	Val216 (4.25), Ser195 (5.61), Gln192 (3.91), Cys58 (4.08; 4.51), His57 (4.74)	His57 (4.91; 5.61), Val216 (4.06), Val99 (5.77)	Phe215, Thr213, Cys191, Ser214, Cys42, Thr41, Arg61, Leu63, Gly193	100	118.75
1-hexadecyl-2-amino-2-deoxy-sn-glycerol	-4.1	Thr41 (3.54)	His57 (4.96), Val216 (3.85; 3.92), Arg217A (6.57), Val99 (5.02)	Phe215, Thr213, Cys42, Gly193, Asp194, Gln192, Ser195, Ser214	100	92.71
1-[1-(4S)-7-(diaminomethylideneamino)-4-[4-(diaminomethylideneamino)butylamino]heptyl]-2-oxopyrimidin-4-yl]-3-methylurea	-6.4	Arg217A (5.84; 6.40), Ser217 (4.75), Thr96 (4.23), Asp60 (3.17; 4.71), Cys191 (4.10)	His57 (6.23), Val99 (4.66)	Gly193, Ser195, Asp194, Gly190, Thr213, Thr226, Gln192, Val216, Phe215, Ser214, Val227, Leu218, Gly219, Thr146, Trp94, Arg61	100	116.66
Dibutyl phthalate	-5.5	Val216 (3.84), Phe215 (5.57)	Phe215 (4.75; 5.26), His57 (7.21), Val216 (4.35; 4.37), Val99 (5.20), Ala99A (4.48), Trp171 (8.05), Arg217A (5.25)	Ser214, Ser195, Gln192, Thr213, Asp194, Gly190, Thr226, Cys191, Thr174, Ser217	75	94.79
Benzenemethanamine	-6.9	Val216 (4.75)	Val99 (4.74), His57 (6.62), Phe215 (6.35), Val216 (4.30)	Ala99A, Thr174, Trp171, Trp94, Ser214, Gln192, Ser195, Arg217A	75	109.375
4,4'-Bis(1-phenylethyl)diphenylamine	-8	Ser195 (6.04)	Trp171 (5.99), Arg217A (5.19; 5.69), Val99 (6.84)	His57, Ser214, Val216, Phe215, Lys224, Leu218, Ser217, Thr174, Gln192, Gly193	100	133.33
Alverine	-5	Ser195 (5.40)	His57 (4.24), Val99 (5.33; 5.94)	Thr96, Trp94, Ser214, Gln192, Cys191, Val216, Phe215	75	89.58
N,N-Dimethylsphingosine	-4.4	Val216 (4.22)	Val99 (5.51; 5.92), Arg217A (4.52; 5.29; 5.93), Phe215 (5.96), Trp171 (5.90; 6.63; 6.77)	Ser214, His57, Ser195, Ser217, Thr174	75	83.33
2-Sulfanylfuro[3,4-d]pyrimidine-5,7-dione	-4	Ser195 (5.58), Gln192 (3.73)	-	Ser214, Phe215, Val216, Cys191, Val99, Gly193, His57	100	91.66

Figure 4



Visualization of the interaction of the test ligands with tyrosinase receptors (2D and 3D) (a) benzocaine; (b) indoleacrylic acid; (c) 7-[2-(1-adamantyl)-2-oxoethyl]-1,3-dimethyl-8-(4-methylpiperazine-1-yl)purine-2,6-dione; (d) withanone; (e) N,N-Dimethyl-4-[(E)-2-(4-pyridinyl)vinyl]aniline; (f) (2E)-2-(Mesitylmethylene)-N-(3-methylphenyl)hydrazinecarbothioamide; (g) perazine; (h) 2-Amino-6-benzyl-3-cyano-4,5,6,7-tetrahydrothieno[2,3-c]pyridine; (i) phenyl(2-pyridinyl)methanone; (j) 1-[1-[(4S)-7-(diaminomethylideneamino)-4-[4-(diaminomethylideneamino)butylamino]heptyl]-2-oxypyrimidin-4-yl]-3-methylurea; (k) benzenemethanamine; (l) 4,4'-Bis(1-phenylethyl)diphenylamine; and (m) alverine.

Figure 5



Visualization of the interaction of the test ligands with the elastase receptor (2D and 3D). (a) indoleacrylic acid; (b) 7-[2-(1-adamantyl)-2-oxoethyl]-1,3-dimethyl-8-(4-methylpiperazine-1-yl)purine-2,6-dione; (c) withanone; (d) cholesteryl acetate; (e) mirtazapine; (f) (2E)-2-(Mesitylmethylene)-N-(3-methylphenyl)hydrazinecarbothioamide; (g) perazine; (h) 2-Amino-6-benzyl-3-cyano-4,5,6,7-tetrahydrothieno[2,3-c]pyridine; (i) 2-((4-Cyclohexyl-5-[1-(dimethylamino)propyl]-4H-1,2,4-triazol-3-yl)sulfanyl)-1-(4-morpholinyl)ethenone; (j) 1-[1-[(4S)-7-(diaminomethylideneamino)-4-[4-(diaminomethylideneamino)butylamino]heptyl]-2-oxypyrimidin-4-yl]-3-methylurea; (k) benzenemethanamine; and (l) 4,4'-Bis(1-phenylethyl)diphenylamine.

Financial support and sponsorship
Nil.

Conflicts of interest

There are no conflicts of interest.

References

- 1 Anandi F, Ferdian PR, Pratiwi J, Amalia RLR, Haerul H, Fitriana N, Nurinsyah AS. Screening of active compounds and LC50 toxicity test of mucus from two land snail species: *Hemiplecta humphreysiana* Lea 1840 and *Amphidromus palaceus* Mousson 1849 as potential nutraceutical preparations. *Zoo Indonesia* 2021; 30:106–116.

- 2 Laneri S, Di Lorenzo R, Sacchi A, Dini I. Dosage of bioactive molecules in the nutraceutical *Helix aspersa* muller mucus and formulation of new cosmetic cream with moisturizing effect. *Nat Prod Commun* 2019; 14:1–7.
- 3 Transparency Market Research. Global Industry Analysis Size Share Growth Trends and Forecast 2014–2020. 2019. Available at: <https://www.transparencymarketresearch.com/pressrelease/global-nutricosmetics-market.htm> [Accessed October 23, 2022].
- 4 El Mubarak MA, Lamari FN, Kontoyannis C. Simultaneous determination of allantoin and glycolic acid in snail mucus and cosmetic creams with high performance liquid chromatography and ultraviolet detection. *J Chromatogr A* 2013; 1322:49–53.
- 5 Cilia G, Fratini F. Antimicrobial properties of terrestrial snail and slug mucus. *J Complement Integr Med* 2018; 15:1–10.
- 6 Selamoglu Z, Dusgun C, Akgul H, Gulhan MF. *In-vitro* antioxidant activities of the ethanolic extracts of some contained-Allantoin plants. *Iran J Pharm Res* 2017; 16:92–98.
- 7 Žitňanová I, Korytár P, Aruoma OI, Sustrová M, Garaiová I, Muchová J, et al. Uric acid and allantoin levels in Down syndrome: antioxidant and oxidative stress mechanisms. *Clin Chim Acta* 2004; 341:139–146.
- 8 Thornfeldt C. Cosmeceuticals containing herbs: fact, fiction, and future. *Dermatol Surg* 2005; 31(7 Pt 2):873–880. discussion 880.
- 9 González Y, Tanaka AS, Hirata IY, del Rivero MA, Oliva ML, Araujo MS, et al. Purification and partial characterization of human neutrophil elastase inhibitors from the marine snail *Cenchrithis muricatus* (Mollusca). *Comp Biochem Physiol A Mol Integ Physiol* 2007; 146:506–513.
- 10 Ulagesan S, Kim HJ. Antibacterial and antifungal activities of proteins extracted from seven different snails. *Appl Sci* 2018; 8:1362.
- 11 Giantari NKM, Prayoga IWI, Laksmiani NPL. Aktivitas pencerah kulit dari katekin secara *in silico*. *J Kimia* 2019; 13:196–200.
- 12 Kim J.H., Byun J.C., Bandi A.K.R., Hyun C, Lee N.H. Compounds with elastase inhibition and free radical scavenging activities from *Callistemon lanceolatus*. *J Med Plant Res* 2009; 3:914–920.
- 13 Garg C, Khurana P, Garg M. Review article: molecular mechanisms of skin photoaging and plant inhibitors. *Int J Green Pharm* 2017; 11:217–232.
- 14 Tribó-Boixareu MJ, Parrado-Romero C, Rais B, Reyes E, Vitale-Villarejo MA, Gonzalez S. Clinical and histological efficacy of a secretion of the mollusk *Cryptomphalus aspersa* in the treatment of cutaneous photoaging. *J Cosmet Dermatol* 2009; 22:247–252.
- 15 Noothuan N, Apitanyasai K, Panha S, Tassanakajon A. Snail mucus from the mantle and foot of two land snails *Lissachatina fulica* and *Hemiplecta distincta* exhibits different protein profile and biological activity. *BMC Res Notes* 2021; 14:138.
- 16 Marwoto RM. Keong darat dari Sumatera (*Moluska Gastropoda*). *Zoo Indonesia* 2016; 25:8–21.
- 17 Nurinsyah AS, Fauzia H, Hennig C, Hausdorf B. Native and introduced land snail species as ecological indicators in different land use types in Java. *Ecol Indic* 2016; 70:557–565.
- 18 Ferdian PR, Handayani TH, Amalia RLR, Nurinsyah AS. Preliminary study on determining alternative feed types from land snails originating in Menoreh, Yogyakarta: *Amphidromus palaceus*, *Dyakia rumphii*, and *Hemiplecta humphreysiana*. *Zoo Indonesia* 2020; 29:151–165.
- 19 Nokinsee D, Shank L, Lee VS, Nimmanpipug P. Estimation of inhibitory effect against tyrosinase activity through homology modeling and molecular docking. *Enzyme Res* 2015; 6:1–12.
- 20 Ambarwati NSS, Azminah A, Ahmad I. Molecular docking, physicochemical and drug-likeness properties of isolated compounds from *garcinia latissima* Miq. on elastase enzyme: *in silico* analysis. *Pharmacogn J* 2022; 14:282–288.
- 21 Ferro S, Deri B, Germano MP, Gitto R, Ielo L, Buemi MR, et al. Targeting tyrosinase: development and structural insights of novel inhibitors bearing arylpiperidine and arylpiperazine fragments. *J Med Chem* 2018; 61:3908–3917.
- 22 Ruiivo EFP, Gonçalves LM, Carvalho LAR, Guedes RC, Hofbauer S, Brito JA, et al. Clickable 4-Oxo- β -lactam-based selective probing for human neutrophil elastase related proteomes. *ChemMedChem* 2016; 11: 1–7.
- 23 Ferdian PR, Elfirta RR, Ikhwan AZN, Haerul K, Sutardi D, Ruhiat G, et al. *In silico* study of phenolic compounds in honey as candidate inhibitors of SARS-CoV-2 Mpro. *Health Res Dev Media* 2021; 31:213–232.
- 24 Lu H-M., Yin D-C., Ye Y-J., Luo H-M., Geng L-Q., Li H-S., et al. Correlation between protein sequence similarity and X-Ray diffraction quality in the Protein Data Bank. *Protein Pept Lett* 2009; 16:50–55.
- 25 Ho BK, Brasseur R. The Ramachandran plots of glycine and pre-proline. *BMC Struct Biol* 2005; 5:14.
- 26 Vinsentria A, Seno D.S.H., Bintang M. *In silico* analysis of *Curcuma longa* against histon asetiltransferase. *Curr Biochem* 2015; 2:43–53.
- 27 Page D, Lattimer J.M., Prakash M, Steiner AW. *Stellar Superfluids*. Oxford: Oxford University Press 2013.
- 28 Du X, Li Y, Xia YL, Ai SM, Liang J, Sang P, et al. Insights into protein-ligand interactions: mechanisms models and methods. *Int J Mol Sci* 2016; 17:1–34.
- 29 Siswanto A, Fudholi A, Nugroho A.K., Martono S. Uji bioavailabilitas tablet floating aspirin. *J Kefarmasian Indones*. 2017; 7:112–119.
- 30 Lipinski CA, Lombardo F, Dominy BW, Feeney PJ. Experimental and computational approaches to estimate solubility and permeability in drug discovery and development settings. *Adv Drug Deliv Rev* 2001; 23:3–25.
- 31 Bickerton GR, Paolini GV, Besnard J, Muresan S, Hopkins AL. Quantifying the chemical beauty of drugs. *Nat Chem* 2012; 4:90–98.
- 32 Raies AB, Bajic VB. *In silico* toxicology: computational methods for the prediction of chemical toxicity. *Wiley Interdiscip Rev Comput Mol Sci* 2016; 6:147–172.
- 33 Fang Y. *Comprehensive medicinal chemistry, III*. Amsterdam: Elsevier; 2017.
- 34 Kroemer RT. Molecular modelling probes: docking and scoring. *Biochem Trans* 2003; 31:980–984.
- 35 Shanmugam S, Kumar TS, Selvam KP. *Laboratory handbook on biochemistry*. New Delhi: PHI Learning; 2010.
- 36 Nurhayati T, Suhartono MT, Nuraida L, Poerwanto SB. Pemurnian dan karakterisasi inhibitor protease dari *Chromohalobacter* sp. 6A3 bakteri yang berasosiasi dengan spons *Xetospongia testudinaria*. *J Teknol Ind Pangan* 2010; 21:143–150.
- 37 Arthur DE, Akoji IN, Sahnoun R, Okafor GC, Abdullahi KL, Abdullahi SA, et al. A theoretical insight in interaction of some chemical compounds as mTOR inhibitors. *Bull Natl Res Cent* 2021; 45:1–12.
- 38 Tiring SSNDT, Bare Y, Mansur S, Maulisi A, Nugraha F A D. Studi *in silico*: prediksi potensi 6-shogaol dalam *Zingiber officinale* sebagai Inhibitor c-Jun N-terminal kinase. *Al-Kimia* 2019; 7:147–153.
- 39 Veeramachaneni GK, Thunuguntla VBSC, Bobbillapati J, Bondili JS. Structural and simulation analysis of hotspot residues interaction of SARS-Cov 2 with human ACE2 receptor. *J Biomol Struct Dyn* 2020; 39:4015–4025.
- 40 Inan S, Oztukcan S, Vatansever S, Ermertcan AT, Zeybek D, Oksal A, et al. Histopathological and ultrastructural effects of glycolic acid on rat skin. *Acta Histochem* 2006; 108:37–47.
- 41 Ehara T, Kitajima S, Kanzawa N, Tamiya T, Tsuchiya T. Antimicrobial action of achacin is mediated by L-amino acid oxidase activity. *FEBS Lett* 2002; 531:509–512.
- 42 Chinaka N, Chuku LC, George G, Oraezu C. Snail slime: evaluation of anti-inflammatory phytochemical and antioxidant properties. *J Complement Altern Med Res* 2021; 13:8–13.
- 43 Ain QU, Khan H, Mubarak MS, Pervaiz A. Plant alkaloids as antiplatelet agent: drugs of the future in the light of recent developments. *Front Pharmacol* 2016; 7:1–9.
- 44 Hanafiah OA, Hanafiah DS, Bayu ES. Quantity differences of secondary metabolites (saponins tannins and flavonoids) from binahong plant extract (*Anredera cordifolia* (Ten.) Steenis) treated and untreated with colchicines that play a role in wound healing. *World J Dent* 2017; 8:296–299.
- 45 Fitriyani A, Winarti L, Muslichah S. Anti-inflammatory test of methanol extract from red betel leaf (*Piper crocatum* Ruiz & Pav) on white rats. *Trad Med J* 2011; 16:34–42.
- 46 Gou L, Jinhyk L, Hao H, Yong-Doo P, Yi Z, Zhi-Rong L. The effect of oxaloacetic acid on tyrosinase activity and structure: integration of inhibition kinetics with docking simulation. *Int J Biol Macromol* 2017; 101:59–66.
- 47 Charissa M, Djajadisastra M, Elya B. Antioxidant and tyrosinase inhibition tests, as well as a benefits test of gel made from Taya (*Nauclea subdita*) bark extract, on the skin. *J Kefarmasian Indosnes* 2016; 6:98–107.
- 48 Wlodarska M, Luo C, Kolde R, d’Hennezel E, Annand J W, Heim C E, et al. Indoleacrylic acid produced by commensal *Peptostreptococcus* species suppresses inflammation. *Cell Host Microbe* 2017; 22:25–37.
- 49 Kacem R. Phenolic compounds from medicinal plants as natural anti-elastase products for the therapy of pulmonary emphysema. *J Med Plants Res* 2013; 7:3499–3507.
- 50 Maulina D. Peran mangiferin sebagai inhibitor enzim kolagenase dan elastase. *Indones J Health Sci* 2021; 1:4–9.
- 51 Wadegaonkar V.P., Wadegaonkar PA. Withanone as an inhibitor of surviving: a potential drug candidate for cancer therapy. *J Biotechnol* 2013; 168:229–233.